KINETICS OF GRAIN GROWTH IN Ti-2.7Al-5.7Fe-6Mo-6V ALLOY

T.D. Mutava *, **L.A. Cornish, I. Sigalas**

School of Chemical and Metallurgical Engineering, University of the Witwatersrand, South Africa, and
DST-NRF Centre of Excellence in Strong Materials, hosted by the University of the Witwatersrand

Abstract

The metastable (βTi) alloy Ti-2.7Al-5.7Fe-6Mo-6V (wt%) was produced by semi-centrifugal casting of blended elemental powders. The phases were identified by X-ray diffraction (XRD), and overall composition was measured by X-ray fluorescence (XRF). The beta transus was determined by differential thermal analysis (DTA) and optical microscopy. The cast alloys were annealed at different temperatures under argon, up to 900ºC, where they were in the solution-treated state, and the solution-treated alloys were aged between 400ºC and 600ºC. The kinetics of grain growth during heat treatment of the as-cast and solution-treated alloys was investigated by metallography, using the grain intercept method. Grain growth depended on whether the matrix was (αTi) or (βTi), and on the competing precipitate dissolution, or nucleation and growth processes. The as-cast alloy had a mean grain size of 19 ± 7µm, which increased to 63 ± 21µm after heat treating at 500ºC for 2h. The alloy was duplex between 590ºC and 800ºC, and completely (βTi) above 800ºC. After solution treatment, the mean grain size was 40 ± 16 µm, which was smaller than at the lower heat treatment temperatures. Following solution treatment, the mean grain size increased with increasing ageing temperature, up to 66 ± 22µm after 2h at 600ºC. The growth exponents were lower than the 0.5 for normal grain growth in both cases, and there was an incubation period at 300ºC and 400ºC when the alloy was not solution-treated. Minimal grain growth was observed close to the beta transus.

Key words: Grain growth; Kinetics; Solution-treatment; Timetal 125.

1. Introduction

Grain size plays a key role in the mechanical properties and performance of polycrystalline materials [1]. Grains have a tendency to grow due to their curvature, as this lowers the surface area to volume ratio and reduces their interfacial energy [1-4]. The growth rate is determined by the grain boundary mobility and the driving force [2], which in turn depends on composition, temperature and prior thermomechanical treatment [4]. It is also generally agreed that there is a threshold grain diameter, above which grains grow, while grains below this threshold are consumed [5]. Since the grain size affects the properties of the material in service [1-7], close control during thermomechanical treatment is important.

In this study, grain growth during heat treatment of cast Ti-2.7Al-5.7Fe-6Mo-6V (wt%), commercially known as Timetal 125 [7], was investigated. It is a metastable (βTi) alloy used as a high strength fastener on aerostructures [1]. Efforts have been made to understand grain growth in titanium alloys and other

polycrystalline materials [4-8]. The investigations ranged from experimental observation and measurement [7, 8] to numerical simulations, such as the Monte Carlo [4, 5] and multi-phase field models [7-9]. While simulations have become well developed for grain growth in single-phase materials, their predictions are less used for multi-phase materials [7]. In all cases, the simulations have always needed to be validated by experimental evidence. So, although they are cheaper and quicker, they are not a substitute for observation of grain growth by metallography.

Gil et al. [10] found that grain growth was faster for (βTi) than for (αTi) in pure titanium. This was attributed to lower activation energy in (βTi), due to easier diffusion in the more open bcc crystal structure, which were 100 kJ.mol-1 in (αTi) and 20 kJ.mol-1 in (βTi). Siemers et al. [11] found the self-diffusion rate to be 2 orders of magnitude higher in (βTi) than in the (αTi) phase, and that grain size in the (βTi) phase can increase by up to 400%.

However, alloy additions and interstitial content were found to have a significant effect on the activation energy for grain growth and kinetics in

titanium alloys [4, 9]. Normally, the presence of alloying elements, in particular chromium and iron, increases activation energy for grain growth, which in turn retards grain growth in titanium alloys. In almost all cases, solute elements segregate to grain boundaries and lower the surface energy of the system. During grain growth, the solute elements lag behind the grain boundaries, creating drag [11]. The activation energy for grain growth in the (βTi) phase was 95 kJ.mol-1 in Ti-6Al-4V [10], and 211 kJ.mol^{-1} in Ti-5.6Al-3.5Zr-1Nb-0.25Mo-0.3Si [9], showing a positive correlation with alloying content. Normal grain growth was observed in commercially pure (CP) titanium between 700°C and 1100°C, with a growth exponent ~0.5, which marginally increased with increasing temperature [4, 8]. However, no growth was found around 900°C, which was attributed to the competing (αTi)-(βTi) transformation, since the temperature was close to the beta transus [8-10]. Grain growth was most rapid in the first 10-15 minutes, and slowed until the mean grain size reached a plateau. This was attributed to the surface area/volume ratio and the interfacial energy between grains, hence driving force, being highest at the start of grain growth and decreasing as the mean grain size increased [7]. Grain growth in pure metals generally follows the parabolic growth law [7, 10, 11], but deviation is observed when other phases are present, particularly when they are small enough to pin the grain boundaries [12-14]. While it is generally agreed that a second phase reduces grain boundary mobility, Shvindlerman and Gottstein [15] showed grain growth can be accelerated by precipitation under the right conditions. This is possible because during precipitation, the grain boundaries become leaner in the solute, which reduces solute drag [15]. If the precipitates are distributed such that they do not pin the grain boundaries, the net effect will be accelerated grain growth. [14].

2. Material and Methods

Commercial grade elemental titanium (99.95 wt%), aluminium (99.95 wt%), iron (99.95 wt%), molybdenum (99.95 wt%) and vanadium (99.95 wt%) powders sourced from Alfa Aeser, South Africa, were blended to manufacture the Timetal 125 composition. Five 40g samples of the blended powders were cold compacted into cylindrical shapes using a bench-top Manfredi hydraulic press, to ensure maximum electrical conductivity. The cold compacts were inductively heated in yttria-stabilised zirconium crucibles in a Manfredi semi-centrifugal titanium casting furnace. The furnace was cyclically purged by drawing a vacuum to -90 kPa and back-filled with high purity argon to atmospheric pressure. The samples were inductively heated using a water-cooled

copper coil, centrifuged into a copper mould, and allowed to cool in the argon-filled casting chamber. The castings, measuring 15 mm diameter and 80 mm length, were sectioned into 3 mm thick discs using a LECO MSX 205A machine, with a 20S30 silicon carbide cutting blade. To avoid burning during cutting, generous amounts of water-based coolant were used, together with a fast wheel speed (3500 rpm) and slow feed rate (0.5 mm.s^{-1}). One as-cast sample was analysed by XRF, XRD and a LECO oxygen analyser. Three sectioned samples were kept in the as-cast condition, while the rest were heat treated in an Elite Thermal Systems TSH 17 muffle furnace, under argon. The castings were further protected by sealing them in quartz ampoules during heat treatment.

In the first set of experiments, heat treatment was done on the cast samples in 100°C increments from 300°C to 800°C for 20, 30, 40, 60, 120, 240 and 300 minutes at each temperature. The samples were quenched in water at 25°C. Subsequently, they were ground using a Manfredi micro-grinder to remove ~5 μm oxidized surface material. Thereafter, they were polished and etched with Kroll's reagent for metallographical analysis, using an Olympus BIOX B51M optical microscope coupled to an Olympus motion stream image analyser. Grain sizes were measured by the grain intercept method.

In the second set of experiments, the cast samples were solution-treated at 900°C for 2 hours and water quenched to retain a fully (βTi) microstructure. These solution-annealed samples were subsequently aged at 400°C, 500°C and 600°C for the same times as in the first set of experiments. Their grain sizes were also determined by the line intercept method, where at least 20 random lines were drawn on the micrographs, and the number of times each line segment intercepted a grain boundary was counted. This was done using the image analyser on the Olympus software, as well as by drawing lines on the micrographs by hand to confirm the accuracy of the image analyser. A total of between 50 and 60 grains were aimed for in each measurement, to obtain a representative measurement. The grain size was calculated from the ratio of intercepts to the line length. The manual intercept counting method gave between 50 and 60 grain sizes from which the mean grain size and the standard deviation were calculated. The grain sizes measured by the image analyzer and the by the manual method were in close agreement.

3. Results

The composition of the as-cast Ti-2.7Al-5.7Fe-6Mo-6V is shown in Table 1.

As-cast Ti-2.7Al-5.7Fe-6Mo-6V contained (αTi) and (βTi), from the XRD pattern in Figure 1. The

Table 1. *Chemical composition of as cast Timetal 125 (wt%), balance is titanium.*

Al	Fe	Mo	V	O	N
2.71	5.7	5.99	6	0.19	0.01

relative XRD peak intensities indicated (αTi) was the major phase, and this agreed with the SEM micrograph in Figure 2. The XRD peaks for (βTi) in the as-cast samples were shifted toward higher angles, compared to pure βTi.

The as-cast alloy contained equiaxed grains, with intergranular and grain boundary precipitates, Figure 2. The intergranular precipitates were richer in iron, molybdenum and vanadium, indicating they were (βTi). It was not possible to separately analyse the grain boundary precipitates by EDS, due to their fine size. The SEM micrograph also showed the as-cast alloy contained porosity, Figure 2.

The optical micrograph of the as-cast sample, Figure 3(a), showed some areas with colonies of (βTi) precipitates, in addition to those on the grain boundaries. After heat treating at 300°C for 60 minutes, the precipitates dissolved, Figure 3(b). However, a new phase precipitated inside the grains after heat treating at 400°C, and persisted to 500°C, but was too fine to measure separately. The sample heat treated at 600°C comprised a mixture of (αTi) and (βTi) grains, but grain measurement was not reliable in this case, due to extensive precipitation. Most of the grain boundaries were masked by the precipitates. A completely different microstructure was observed after heat treatment at 800°C, Figure 3(e). XRD showed the major phase after heat treating at 800°C was (βTi), indicating the temperature was close to, and marginally above, the beta transus. This was supported by differential thermal analysis (DTA),

which showed the (α+β) phase region was between 590°C and 800°C. The light grain boundary precipitates were determined to be (αTi) by EDS, although they were too small to analyse accurately.

The mean grain size in the as-cast condition was $19 \pm 7\mu m$, which increased after heat treatment, as shown in Figures 3 and 4. Generally, there was an increase in the mean grain size with increasing temperature and time, until it reached a plateau after ~40 minutes, Figure 4. The growth was rapid in the first 20 minutes, although there was an incubation period at 300°C and 400°C, as indicated by the delayed growth at these temperatures. In the first 5 minutes, the mean grain sizes at the two temperatures were approximately the same, as shown by the overlaying curves. Beyond this, the mean grain size was larger at 400°C than 300°C for each heat treatment period, but more pronounced growth was observed after heat treating at 500°C. At 800°C, grain
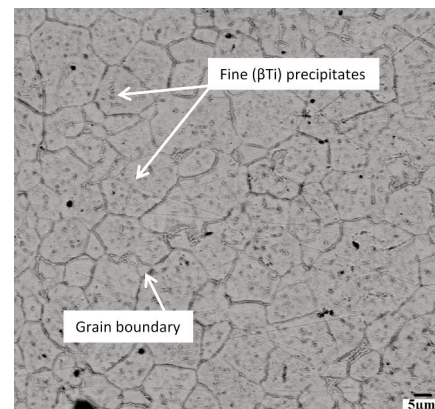

Figure 2. *SEM-BSE image of Timetal 125 in the as-cast condition showing intergranular and grain boundary precipitates and porosity (micron bar = 5µm).*

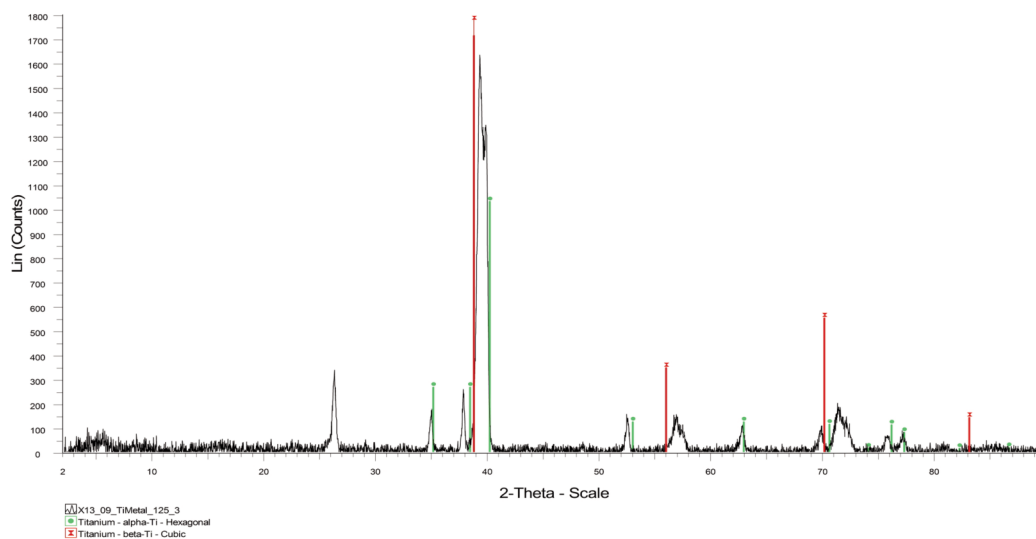**Figure 1.** *XRD pattern of Timetal 125 in the as-cast condition.*
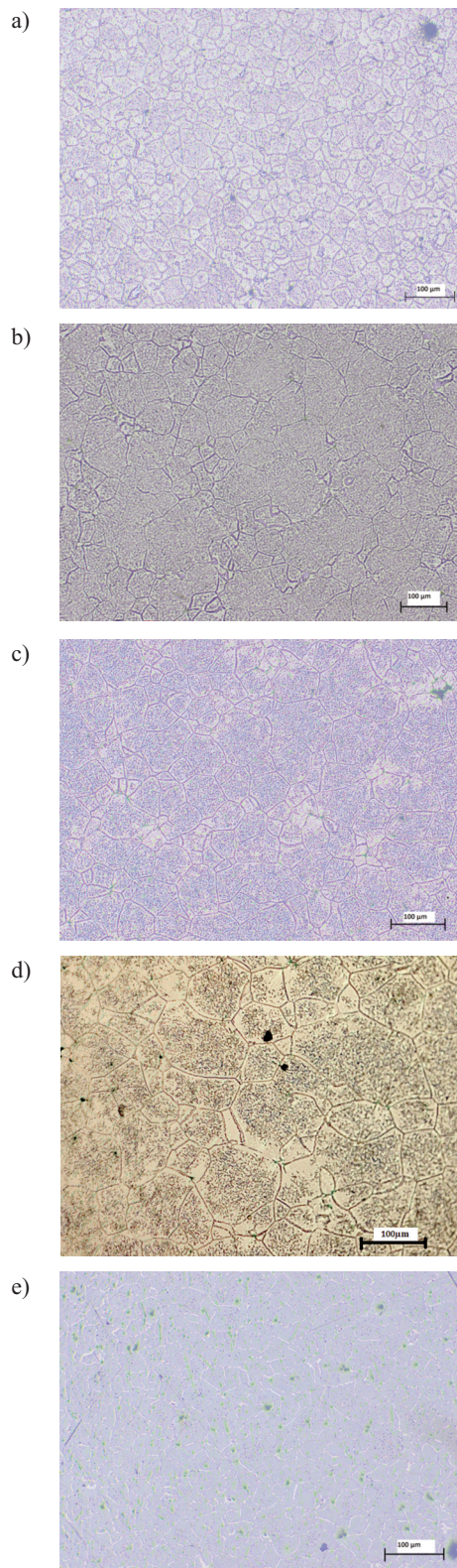
a)

b)

c)

d)

e)

Figure 3. Optical micrographs showing the grain sizes of (a) the as-cast alloy, and after heat treating for 60 minutes at (b) 300ºC, (c) 400ºC, (d) 500ºC and (e) 800ºC.

growth was very rapid initially, but the mean grain size was only marginally larger than at 500ºC.

The beta transus of the alloy was determined to be 800ºC using DTA, XRD and metallography. After water quenching from 900ºC, the alloy was almost completely (βTi) with a few precipitates along the grain boundaries, Figure 5(a), showing it was in the solution-treated state. The mean grain size was $40 \pm 3\mu m$, which was smaller than at 800ºC. The presence of the (αTi) on the grain boundaries after solution treatment indicated that the quenching was rapid enough to completely suppress the partial transformation of (βTi) to (αTi). The microstructure after solution treatment (Figure 5 (a)) was very similar to that at 800ºC in Figure 3 (e), because the two heat treatments were in the same phase field.

After ageing, the (αTi) precipitates became more distinct, and coarsened with increasing temperature and time. Some of the precipitates coarsened into allotriomorphs, Figures 5(c) and (d). In addition to the grain boundary precipitates, there were also some finer precipitates inside the grains, and the amount of these precipitates increased with increasing ageing temperature. The variation of the mean grain size with temperature and time after solution-treatment and ageing is shown in Figure 6. The mean grain size increased with increased with ageing temperature from 400ºC to 600ºC. The initial grain growth rate was not as rapid as during annealing. However, like annealing, the mean grain size reached a plateau after about 40 minutes.

4. Discussion

Isothermal grain growth normally follows the Hillert model, as used by Iqbal et al. [8], shown in Equation 1, where d is the mean grain diameter, d_o is the initial mean grain diameter, k is a rate constant, t is time and n is the growth exponent, usually ~0.5 for normal grain growth [4, 16]:

$$d = d_o + kt^n \tag{1}$$

A plot of $\ln(d-d_o)$ against $\ln(t)$ should be linear, with the vertical intercept equal to $\ln(k)$ and slope to the growth exponent, n. Gil et al. [10] argued that k is of the Arrhenius type, shown in Equation 2, since atomic diffusion across a grain boundary is a simple thermally-activated process:

$$k = k_o e^{\frac{-E_a}{RT}} \tag{2}$$

where k_o is a pre-exponential factor independent of temperature, T is the absolute temperature, E_a is the activation energy for grain growth and R is the universal gas constant. A plot of $\ln(k)$ against $(-1/T)$ should also be linear with a slope equal to E_a/R and vertical intercept equal to $\ln(k_o)$. The $\ln(d-d_o)$-$\ln(t)$ plots after heat treating Timetal 125 are shown in
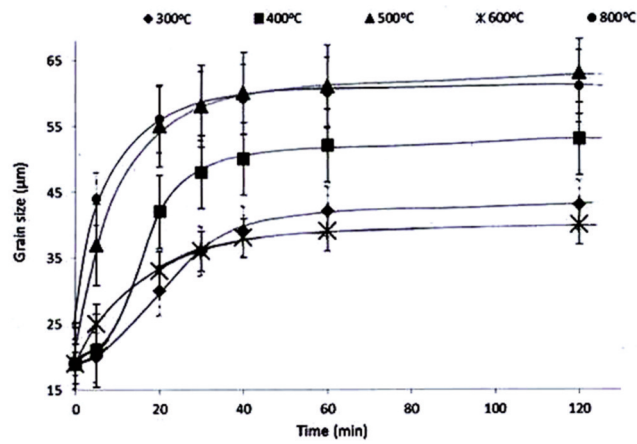
Figure 4. Grain size as a function of temperature and time during heat treatment of the cast Timetal 125.
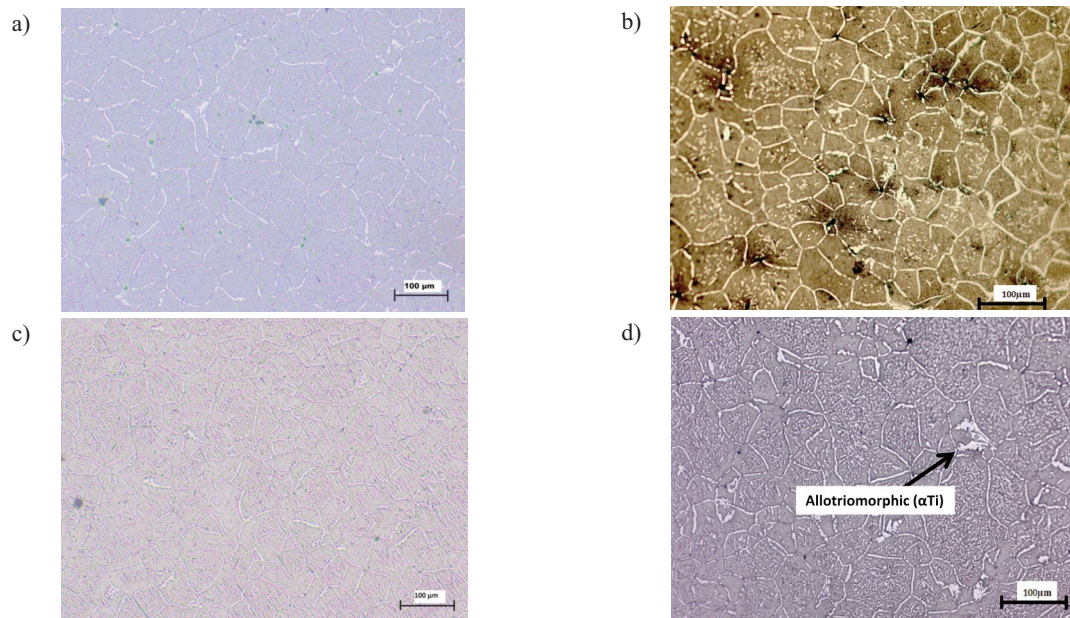

*Figure 5. Optical micrographs of Timetal 125 after
(a) solution-treatment, and solution-treatment and ageing for 60 min at (b) 400ºC, (c) 500ºC and (d) 600ºC.*
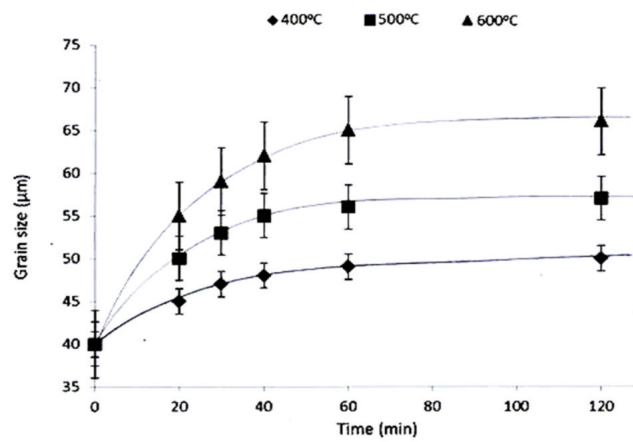

Figure 6. Mean grain size of size after solution-treatment at 900ºC and ageing at different temperatures.

Figure 7. The plots are linear at 500°C and 800°C, but the fits were poor at the lower temperatures. The poorer linear correlation at 300°C and 400°C is consistent with the incubation period in Figure 4.

Figure 8 shows similar plots, after solution-treatment and ageing. Based on the regression coefficients, the plots were less linear than in Figure 7, and the slopes after solution treatment and ageing were generally larger than for annealing. The highest growth exponent was 0.39 at 400°C, but smaller at 500°C and 600°C. The larger growth exponents were attributed to a lower activation energy for grain growth in the (βTi) matrix. The smaller exponents at the higher ageing temperatures were due to the competing (αTi) precipitation and its coarsening, Figures 5(b)-(d). The small grain size after ageing at 600°C was not consistent with the generally increased grain size with increasing ageing temperature, which was attributed to nucleation of (βTi) from the (αTi), since this was above the beta transus of the alloy.

The matrix after solution-treating was different from the as-cast state. In the as-cast condition, the alloy had an (αTi) matrix and colonies of (βTi) precipitates, while after solution-treatment, the matrix was (βTi) and the precipitates were (αTi). Therefore, the mechanisms of grain growth were different, due to the difference in the activation energy for grain growth because of the dissimilar crystal structures [9, 13-15]. The (α+β) phase boundaries were determined to be 590°C and 800°C by DTA. The beta transus (800°C) was higher than reported by Leyens and Peters [9] for the same alloy (760°C), which was attributed to the 0.3 wt% oxygen in the cast samples, since interstitials appreciably increase the transformation temperature.

In both sets of experiments, the rapid increase in grain size in the first 20 minutes was due to the high surface energy/volume ratio initially, and as this decreased as the grains grew, the ratio and driving force also decreased, which agreed with Gil et al. [10]. The increase in the mean grain size of the (αTi) matrix between 300°C and 500°C was in response to the increasing thermal energy. The incubation period at 300°C and 400°C was because part of the thermal energy was used to dissolve the initial precipitates, Figures 3(a) and (b), although other factors like pinning precipitates, too small to resolve under an optical microscope, may have had an influence. This also explains the poorer linear correlations in the plots in Figure 7 at 300°C and 400°C. The lack of incubation at 500°C and 800°C, as supported by the more linear plots at these temperatures and the rapid initial grain growth in Figure 4, indicated there was enough energy to simultaneously support the dissolution of the precipitates and grain growth.

The similarity of grain sizes at 300°C and 400°C was due to the competing precipitation reaction, Figures 3(b) and (c). A significant amount of the thermal energy was expended in precipitating the new phase at the expense of grain growth, since phase transformations lower the Gibbs energy much more than the decrease in surface energy from growing grains [13]. Since the precipitation occurred in the 300°C to 400°C interval, the precipitates after heat treating at 500°C should have formed in the same temperature interval. (The (α+β) phase region was determined to be between 590°C and 800°C by DTA and metallography.) Therefore, the extra thermal energy from increasing the temperature from 400°C to 500°C was mainly used for grain growth, explaining the significant increase in grain size in this temperature interval. The smaller mean grain size was attributed to the (αTi)-(βTi) transformation occurring at the expense of grain growth. Additionally, the β
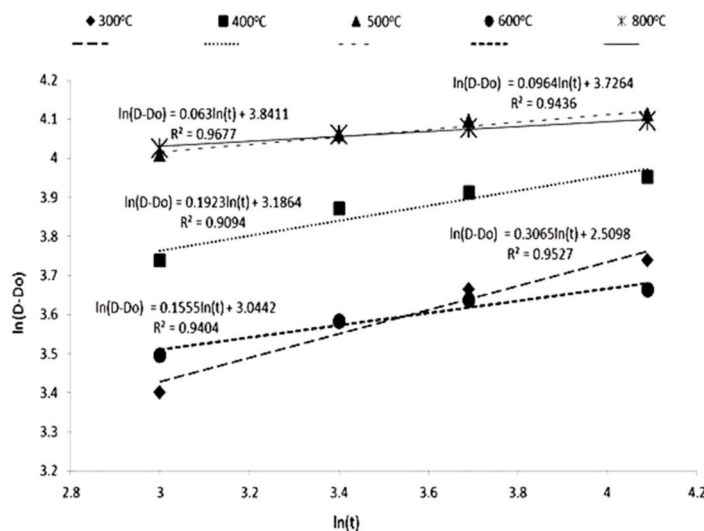

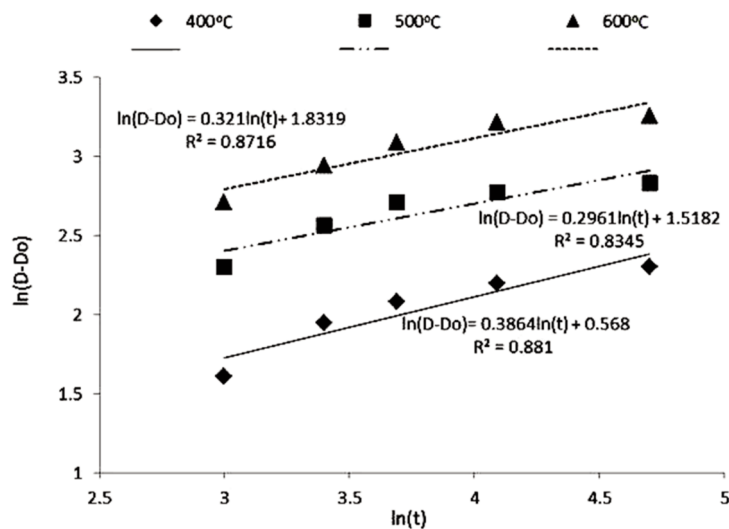*Figure 7. ln(d-d$_o$) against ln(t) after annealing the cast Timetal 125 at different temperatures.*

Figure 8. ln(d-do) vs. ln(t) solution-treatment and ageing at different temperatures.

phase was expected to be small, since it was nucleating on the many pre-existing (αTi) grains. Also, the apparent lack of grain growth at 800°C was also because most of the thermal energy was used for the (αTi)-(βTi)transformation, since heat treatment was at the beta transus, which agreed with Gil et al. 10] for CP titanium. Furthermore, the transformed (βTi) grains would have been very small initially, and would take time to grow.

During ageing, the mean grain size increased with temperature and time, Figure 6. However, at and above the (βTi) transus, the grains would be expected to be small, since they would have nucleated on the existing (αTi) grain boundaries before growing. The smaller than expected grain growth at the higher ageing temperatures was attributed to increasing precipitation of the (αTi) phase, which competed for the available energy. Furthermore, the coarsening of the grain boundary precipitates may have affected the accuracy of measuring the grain sizes at the higher ageing temperatures.

The growth exponents, obtained from the slopes in Figures 7 and 8, were all less than 0.5, indicating grain growth was not normal. However, Kim et al. [4] argued normal grain growth has been observed in materials where n≠0.5, and that the distribution of the small grains determines the exponent's value. The similarity of the growth exponents at 300°C (n ~0.3) and 400°C (n ~0.2) during heat treatment of the cast alloy was due to the similarity in grain sizes and microstructures at the two temperatures. The very low growth exponents at 500°C (n ~0.1) and 800°C (n ~0.06) were attributed to increased solute drag due to solute enrichment of the matrix as the (βTi) precipitates dissolved [1,16-21]. The growth exponents during ageing were also smaller than 0.5 at all the test temperatures, which was attributed to

significant solute drag, since all the alloying elements were dissolved in the matrix after solution-treatment. Additionally, part of the available thermal energy was used to precipitate and coarsen the (αTi) phase. Unlike the (βTi) precipitates, which simply dissolved during the heat treatment of the cast alloy, the (αTi) precipitates obtained after ageing grew. In addition to expending energy, the precipitates grew and coarsened on the grain boundaries at the expense of the matrix's volume [20]. In effect, the mean grain sizes after ageing may have been marginally larger than recorded, due to the masking effect of the coarse precipitates, which is a weakness of the grain intercept method in multi-phase alloys [21].

There is another complication in that the interdiffusion coefficients of the elements would also have an effect on grain growth. For example, Wang et al. [22] found that for Al in the α_2 Ti_3Al phase with Nb, there was a maximum in the ternary interdiffusion coefficient of Al in Ti (strictly Ti-Ti for the ternary calculation [23]) and a corresponding minimum of that for Al in Nb (strictly Nb-Nb in the ternary calculation) at approximately 4 at.% Nb. Although the alloy in the current study is different (in terms of both composition and structure), Wang et al. [22] showed that the diffusivities also had a more complex behaviour, rather than just increasing/decreasing monatomically, and the compositions of Fe, Mo and V could fall in this range. This variation also adds to the complexity of the grain sizes, because there are two competing phases in the phase transition.

5. Conclusions

Blended elemental powders were successfully consolidated by semi-centrifugal casting, and heat treated to form Ti-2.7Al-5.7Fe-6Mo-6V alloys. XRD

showed the as-cast alloy contained both (αTi) and (βTi), and EDS indicated the matrix was the (αTi) phase. From DTA and metallography, the alloy was (α+β) between 590ºC and 800ºC, and completely (βTi) above 800ºC. The kinetics of grain growth during heat treatment was quantified by metallography, using the grain intercept method. The growth kinetics depended on whether the matrix was (αTi) or (βTi), as well as on the presence of secondary phases. Minimal incubation was required in the (βTi) phase, suggesting growth was easier than for the (αTi) matrix, due to the more open bcc crystal structure of (βTi). During heat treatment of the cast sample, grain growth competed with the dissolution of the (βTi) precipitates, while during ageing of the solid solution samples, the nucleation and growth of the (αTi) precipitates were competing processes. There was minimal grain growth close to the beta transus because of the competing (αTi)-(βTi) transformation. The mean grain size after heat treating above the transus was smaller than at the lower temperatures, because the (βTi) phase nucleated on the many pre-existing (αTi) grain boundaries. The growth exponents were generally smaller than reported for normal grain growth, due to significant solute drag and the presence of a secondary phase.

References

[1] J.P. Hirth, J. Lothe, Theory of dislocations, Krieger, Malabar, Florida, USA, (1968).

[2] D.A. Molodov, C. Bollmann, P.J. Konijnenberg, L.A. Barrales-Mora, V. Mohles, Mater. Trans., 48 (11) (2007) 2800-2808.

[3] I. Steinbach, F. Pezzolla, B. Nestler, M. Seesselberg, R. Prieler, G.J. Schmitz, J.L.L. Rezende, Phys. D. 94 (1996) 135-147.

[4] B.N. Kim, N.M. Hiraga, K. Morita, Mater. Trans., 44 (11) (2003) 2239-2244.

[5] Y. Tan, A.M. Maniatty, C. Zheng, J.T. Wen, Model. Simul. Mater. Sci. Eng., 25 (6) (2017) 1947-52.

[6] A.M. Deus, M.A. Fortes, P.J. Ferreira, J.B. Vander Sande, Acta Mater., 50 (2002) 3317–3330.

[7] M.J. Tan, X.J. Zhu, J. Achiev. Mater. Manuf. Eng., 18 (1-2) (2006) 183-186.

[8] N. Iqbal, N.H. van Dijk, S.E. Offerman, M.P. Moret, L. Katgerman, G.J. Kearley, Acta Mater., 53 (2005) 2875-2880.

[9] C. Leyens, M. Peters, (Eds.) Titanium and Titanium Alloys: Fundamentals and Applications, (2003), WILEY-VCH Verlag GmbH & Co. Kga A, Wiehneim, Germany, pp. 38-65.

[10] F.J. Gil, D. Rodriguez, J.A. Plannel, Scr. Metall. Mater., 33 (8) (1995) 1361-1366.

[11] C. Siemers, F. Brunke, M. Starche, J. Laukart, B. Zahra, J. Rosler, P. Rockiki, K. Saksl, Proceedings of the 11th World Conference on Titanium (Ti-2011), Beijing, China, (2011).

[12] T. Takaki, A. Yamanaka, Key Eng. Mater., 626 (2015) 81-84.

[13] Y. Huang, F.J. Humphreys, Mater. Chem. Phys., 132 (2012) 166-174.

[14] D. Raabe,, Comput. Mater. Sci., (1998), Wiehneim, Wiley-VCH.

[15] L.S. Shvindlerman, G. Gottstein, Scr. Mater., 50 (2004) 1051-1054.

[16] R. Reinbach, A. Nowikow, Z. Metallkunde, 47 (1956) 583-584.

[17] F.J. Gil, J.M. Manero, J.A. Planell, Effect of Heat Treatment on the Cyclic Softening of Ti-6AI-4V Alloy, F.H. Frees, I.L. Caplan, (Eds.), The Minerals, Met. Mater. Soc., (1993), pp. 1843-1850.

[18] J. Pask, A. Evans, Mater. Sci. Res., 14 (1980) 167-189.

[19] M. Krośniak, P. Pałka, G. Boczkal, Key Eng. Mater., 682 (2016) 107-112.

[20] S.L. Semiatin, J.C. Soper, I.M. Sukonnik, Scr. Metall. Mater., 30 (7) (1994) 951-955.

[21] P.R. Rios, Acta. Metall., 35 (12) (1987) 2805-2814.

[22] W. Wang, B. Yuan, C. Zhou, J. Min. Metall. Sect. B-Metall., 48 (2) B (2012) 283 – 290.

[23] M. A. Dayananda, Metall. and Mat. Trans. A, 27 (1996) 2504-2509.